Effect of Bi bilayers on the topological states of Bi_2Se_3: A first-principles study

K. Govaerts,[1,*] K. Park,[2] C. De Beule,[3] B. Partoens,[3] and D. Lamoen[1]
[1]*EMAT, Universiteit Antwerpen, Groenenborgerlaan 171, 2020 Antwerpen, Belgium*
[2]*Department of Physics, Virginia Tech, Blacksburg, Virginia 24061, USA*
[3]*CMT Group, Department of Physics, Universiteit Antwerpen, Groenenborgerlaan 171, 2020 Antwerpen, Belgium*
(Received 24 July 2014; revised manuscript received 19 September 2014; published 20 October 2014)

Bi_2Se_3 is a three-dimensional topological insulator which has been extensively studied because it has a single Dirac cone on the surface, inside a relatively large bulk band gap. However, the effect of two-dimensional topological insulator Bi bilayers on the properties of Bi_2Se_3 and vice versa, has not been explored much. Bi bilayers are often present between the quintuple layers of Bi_2Se_3 , since $(Bi_2)_n(Bi_2Se_3)_m$ form stable ground-state structures. Moreover, Bi_2Se_3 is a good substrate for growing ultrathin Bi bilayers. By first-principles techniques, we first show that there is no preferable surface termination by either Bi or Se. Next, we investigate the electronic structure of Bi bilayers on top of, or inside a Bi_2Se_3 slab. If the Bi bilayers are on top, we observe a charge transfer to the quintuple layers that increases the binding energy of the surface Dirac cones. The extra states, originating from the Bi bilayers, were declared to form a topological Dirac cone, but here we show that these are ordinary Rashba-split states. This result, together with the appearance of a new Dirac cone that is localized slightly deeper, might necessitate the reinterpretation of several experimental results. When the Bi bilayers are located inside the Bi_2Se_3 slab, they tend to split the slab into two topological insulators with clear surface states. Interface states can also be observed, but an energy gap persists because of strong coupling between the neighboring quintuple layers and the Bi bilayers.

DOI: 10.1103/PhysRevB.90.155124 PACS number(s): 73.20.At, 71.20.−b, 71.70.Ej

I. INTRODUCTION

Topological insulators (TIs) are materials with conducting surface states that are protected by time-reversal symmetry [1–3] and a bulk band gap. These states emerge from a combination of band inversion caused by strong spin-orbit coupling (SOC) and time-reversal symmetry leading to an odd number of Dirac-like dispersions between time-reversal-invariant k points. The $(Bi,Sb)_2(Te,Se)_3$ compounds are a well-known family of three-dimensional TIs [4], of which Bi_2Se_3 is the ideal candidate for the study of Dirac surface states, because it has a single Dirac cone on the surface, located inside the bulk band gap, which is relatively large ($\sim$0.3 eV [5–8]).

Freestanding ultrathin Bi films of two to three bilayers were theoretically proposed to be two-dimensional TIs [9–11]. However, ultrathin Bi bilayers are difficult to grow without a substrate, so it is important to understand the effect of the substrate on the electronic structure, and especially the topological edge states, of the Bi bilayers. In this regard, there have been several experimental and theoretical reports of ultrathin Bi bilayers on various substrates [12–14] and of the effect of strain on Bi bilayers [11,15]. One family of suitable substrates are $(Bi,Sb)_2(Te,Se)_3$ compounds, considering their small lattice mismatch. Previous studies showed that a single Bi bilayer becomes metallic when placed on Bi_2Se_3 or Bi_2Te_3, and yet forms Dirac states due to interactions with the TI surface states [13,14,16,17]. Moreover, it has been shown experimentally [18–20] and theoretically [21,22] that a homologous series of $(Bi_2)_n(Bi_2Se_3)_m$ form stable ground-state structures when the Bi concentration is over 40% (or for the Bi-rich phase). As a result, thin Bi bilayers may coexist with Bi_2Se_3 quintuple layers (QLs).

The interaction between neighboring QLs is of a weak van der Waals (vdW) type, so that cleaving of the crystal along the [111] direction can take place between two QLs with Se termination. However, a recent study [23], based on experiment and *ab initio* calculations reveals a complete Bi termination at room temperature, consistent with a Bi bilayer on top of the nominal surface. In addition, this structure was observed to be energetically favorable over the Se-terminated structure. Despite a more complex band structure, the study suggested that the topological surface states migrate to the Bi bilayer. However, this result is inconsistent with another similar experiment indicating only Se-terminated Bi_2Se_3 [24].

In this work, we address the following questions that were raised based on the stable Bi-rich homologous series and on the controversy regarding the surface termination: If Bi bilayers coexist with a Bi_2Se_3 slab, where are they positioned, and which configurations out of a Bi-terminated TI slab and a TI slab with Bi bilayers inside, are energetically favorable? What are the consequences for the topological states of Bi_2Se_3 if Bi bilayers are present? If the Bi bilayers are inside a Bi_2Se_3 slab, do they split the TI into two TIs with extra protected interface states? Where are the protected Dirac states localized? To answer these questions, we investigate the electronic structure of different sequences of Bi bilayers and Bi_2Se_3 QLs, using *ab initio* methods. We focus on the binding energy of the Dirac states, which is defined by the difference in energy between the Fermi level and the Dirac point [25–28].

Our *ab initio* calculations show there is no distinction in the stability of Bi bilayers when they are inside a Bi_2Se_3 slab or at the surface. When Bi bilayers are at the surface of a Bi_2Se_3 slab, the Bi bands exhibit large Rashba spin splitting due to the charge transfer from the Bi bilayer to the slab, and three Dirac cones are formed. When the Bi bilayers are inside the slab, they tend to split the TI into two TIs, only leading to an increased binding energy of the original surface states.

*kirsten.govaerts@uantwerpen.be

However, the interface states never form a Dirac cone, even if we increase the number of Bi bilayers, due to the strong coupling between the neighboring QLs and the Bi bilayers.

II. COMPUTATIONAL METHODS

First-principles calculations were performed within the density-functional theory (DFT) formalism as implemented in the Vienna *ab initio* simulation package VASP [29,30]. We used the all-electron projector augmented wave (PAW) method with the Bi ($6s^2 6p^3$) and Se ($4s^2 4p^4$) electrons treated as valence electrons. The generalized-gradient approximation of Perdew-Burke-Ernzerhof (PBE) [31] was used to describe the exchange and correlation interaction. Since the vdW interaction is known to be important in Bi-Se compounds, we include it by using the optB86b-vdW density functional as implemented in the VASP code [32]. A plane wave cutoff value of 300 eV and a $16 \times 16 \times 1$ grid [33] for the Brillouin zone integration were used for calculating the total energy and structural relaxation.

Bare (111) slabs of four to five QLs were modeled with a vacuum of $\sim$20 Å, and by relaxing both the lattice parameters and atomic positions. This resulted in an in-plane lattice parameter $a = 4.1749$ Å for the bare four QLs and $a = 4.1616$ Å for the five QL slab, while the bulk value is $a = 4.1616$ Å. For the slab with extra layers on top of the surface, we used the same amount of vacuum and only relaxed the atomic positions of the original top QL and the superimposed layers. Convergence is achieved when the forces between the relaxed atoms are less than 5 meV/Å. The SOC was included self-consistently for the final total energy and band structure calculations.

III. RESULTS AND DISCUSSION

Experiment has shown that the energy gap opens when Bi_2Se_3 is thinner than six QLs because of the hybridization between the two surfaces [34]. First-principles studies show that a slab of four QLs is sufficient to close the gap at the Γ point because the distribution of the wave functions is localized strongly in the surface region, with a decay length of one to two QLs [28,35,36]. Moreover, Ref. [28] shows that even for a slab containing two QLs, single-side adsorption leads to two shifted Dirac cones. It is therefore sufficient to consider slabs of four and five QLs, making the calculations computationally feasible.

A. Energetics of different structures

We consider structures of four and five QLs with one or two Bi bilayers in the following three stacking configurations: (i) when the bilayers are located at the surface [Fig. 1(a)], (ii) underneath the first QL [Fig. 1(c) without a vacuum gap], (iii) or underneath the second QL [Fig. 1(d)]. The energy of the different stackings with a fixed number of Bi_2Se_3 QLs and Bi bilayers are compared to resolve the previous contradictory results [23,24] regarding the (111) surface termination of Bi_2Se_3. However, structures with the same number of QLs and bilayers show only a very small difference in energy ($<$10 meV/atom), showing that there is no particular position of the Bi bilayer that is experimentally favored. We should remark that we did not investigate the effect of different stacking patterns on the stability of the structures, nor on the electronic band structure. Although different stackings might influence these properties [37,38] it is beyond the scope of this study, where only $ABCABC$ stackings are investigated.

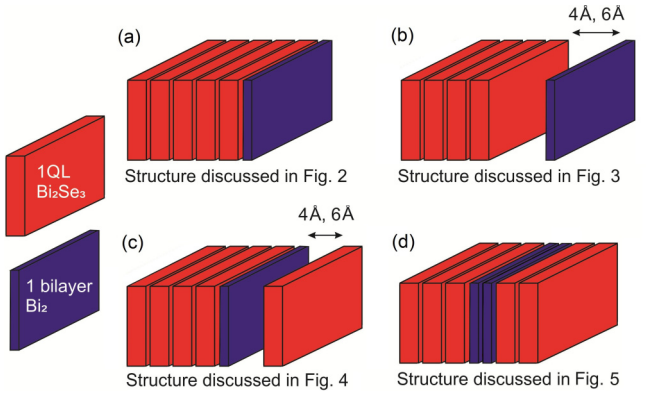

FIG. 1. (Color online) Schematic illustration of the examined structures. The thick red blocks represent Bi_2Se_3 QLs, while the thin blue blocks represent Bi bilayers.

Bi-terminated structures are interesting because Bi_2Se_3 is a good substrate for Bi bilayers. Previous ARPES experiments and DFT calculations on Bi-terminated structures suggest that the electronic structure of both materials is strongly affected by the Bi-TI interaction [13,14,23,24]. Furthermore, there are no systematic studies on the topological surface states in both the Se-terminated and Bi-terminated TI slabs with Bi bilayers. Thus, henceforth, we examine the electronic structure and, in particular, the Dirac surface states of the different stacking configurations.

B. Bi bilayers on top of Bi_2Se_3

We consider a Bi_2Se_3 slab of five QLs and add one Bi bilayer on top, $(Bi_2Se_3)_5(Bi)_2$, as shown in Fig. 1(a). The atomic positions of the topmost QL and the Bi bilayer are relaxed with the rest of the atoms fixed. Figure 2(c) shows the band structure of $(Bi_2Se_3)_5(Bi)_2$, while Fig. 2(a) corresponds to the bare five QL slab, $(Bi_2Se_3)_5$. To identify the contributions of the different QLs or bilayers in the band structure, the electron densities were projected on the individual atomic layers. The blue and red colors in the band structures of Fig. 2 indicate that more than 40% of the electron density corresponding with this level comes from the topmost or bottommost QL of the bare slab, respectively [39]. Orange circles represent states of which more than 30% of the electron density is located in the superimposed Bi bilayer. In Fig. 2(c), apart from several Rashba-split quantum-well states in the valence and conduction band, four Dirac-like cones can be observed, which are labeled 1 to 4. Figure 2(d) shows the layer-projected electron densities of these states at Γ. It is clearly seen that state 1 originates from the superimposed Bi_2 and states 3 and 4 from the lower and upper QL, respectively. The electron density of state 2 mainly comes from a quantum-well state localized at the midpoint between the first and the second QL. In the presence of the Bi bilayer, we observe a downward shift of the Dirac cone for both the top surface state (labeled as state

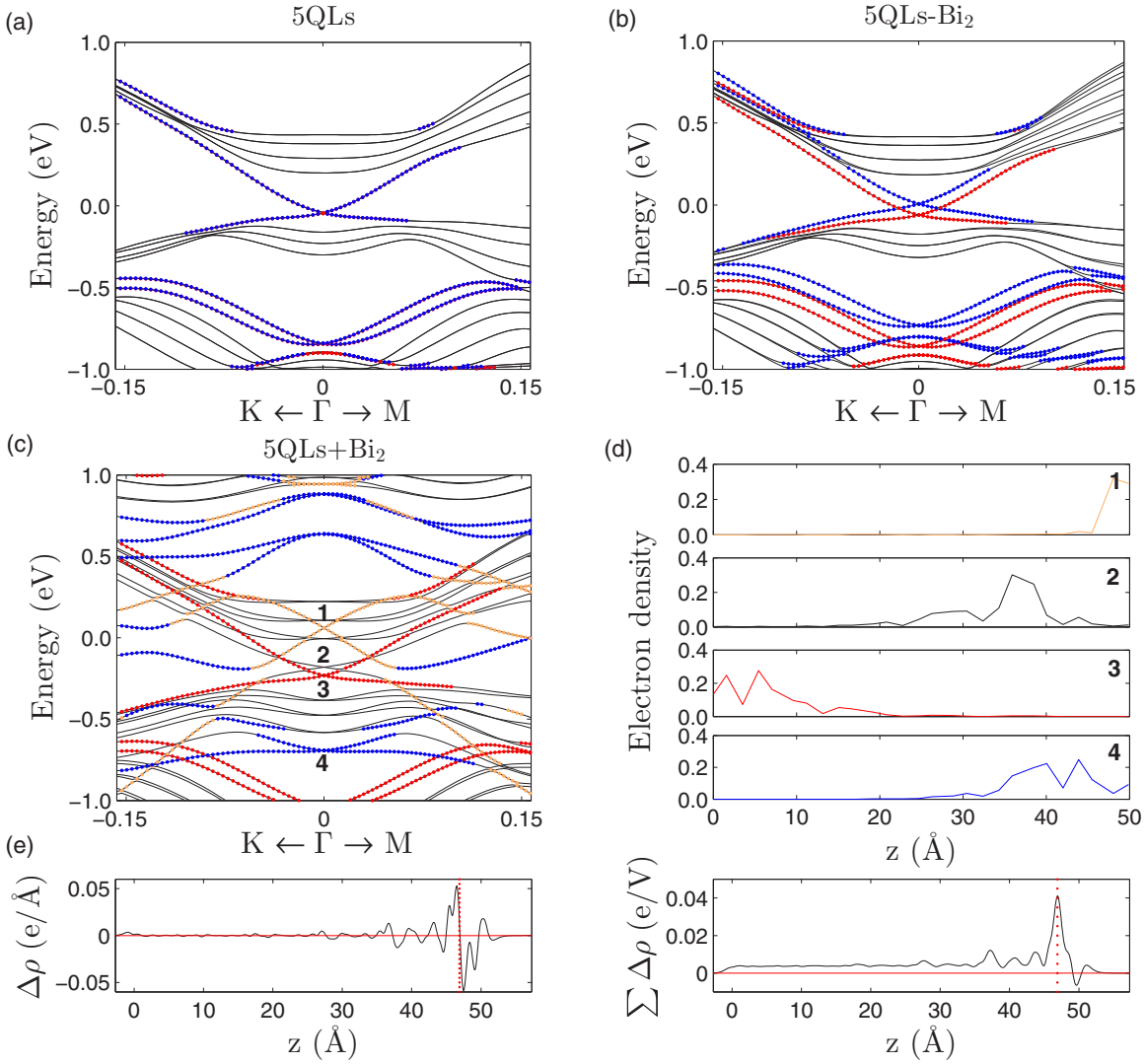

FIG. 2. (Color online) Band structures of (a) a bare slab of five QLs Bi_2Se_3, (b) the same five QLs but in the relaxed coordinates of the five QL system with an extra Bi bilayer on top, and (c) five QLs with a Bi bilayer on top. (d) The layer-projected electron densities of the states 1–4 labeled in (c) at Γ. (e) The charge-transfer amount of the system with five QLs and a bilayer. The right-hand-side figure in (e) is the accumulated charge-transfer amount. The red dotted vertical line denotes the middle between the QLs and the bilayer.

4) and the bottom surface state (labeled as state 3), consistent with an increase in the binding energy ($E_B = E_F - E_{DP}$) of these Dirac cones. The bands coming from the Bi bilayer [orange in Fig. 2(c)] appear near the Fermi level (labeled as state 1).

The origin of the increased binding energies is twofold: It is the combination of a structural relaxation effect with charge transfer from the Bi bilayer to the Bi_2Se_3 slab. Figure 2(b) shows the band structure of the five QL slab where the bare slab is kept in the relaxed coordinates of the $(Bi_2Se_3)_5(Bi)_2$ but the Bi bilayer is removed. The slight relaxation of the top surface leads to an increased binding energy of the bottom surface cone, while the top cone becomes unoccupied. Adding the Bi bilayer now increases the binding energy of the top cone significantly due to a charge transfer from the Bi bilayer to the Bi_2Se_3. Remarkably, we also observe a downward shift of the bottom cone; this would mean the charge transfer extends all the way to the bottom QL. To justify our findings, the amount of charge transfer is calculated by subtracting the electron densities of the extra Bi bilayer and of the bare QLs from the total electron density of the relaxed system. The electron densities are all obtained from the same unit cell, atomic positions, parameter values, and k-point sampling. Figure 2(e) shows the amount of charge transfer of $(Bi_2Se_3)_5(Bi)_2$ on the left and the accumulated amount of this charge transfer on the right. Note that the charge transfer does indeed extend all the way to the bottom QL of the slab. We find that 0.039 electrons per unit cell area are transferred from the bilayer to the QLs, of which 0.027 electrons are transferred to the top QL and 0.0038 electrons to the bottom QL. A simple density of states calculation for a Dirac cone with group velocity $\sim 5.0 \times 10^5$ m s^{-1} of Bi_2Se_3 [1,3] shows that such a small charge transfer can indeed lead to an increased binding energy of 0.2 eV [28].

We also investigate the influence of two Bi bilayers on the electronic properties of the bare slab and conclude that apart from a small shift of bands, the overall band structure of

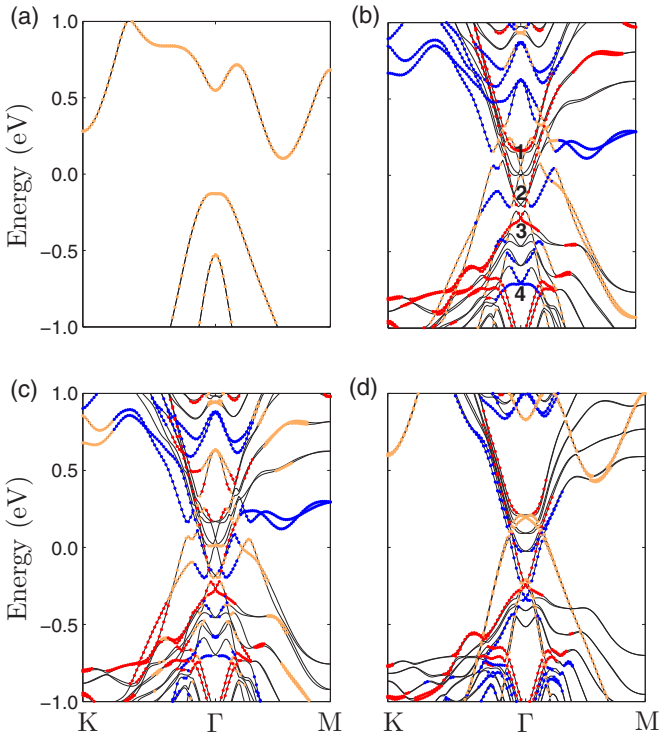

FIG. 3. (Color online) Band structures of (a) a single Bi bilayer, (b) four QLs with a bilayer on top in the relaxed atomic positions, (c) four QLs with a bilayer at 4 Å and (d) at 6 Å vertical distance.

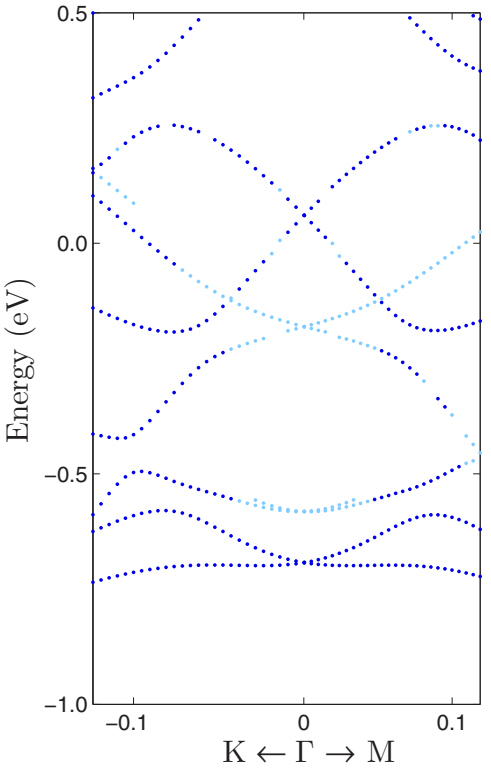

FIG. 4. (Color online) Projected band structure of five QLs with a Bi bilayer on top. Here only the projection on the upper two QLs and the Bi bilayer are shown in order to compare with ARPES data. When more than 90% of the electron density comes from these layers, it is indicated in dark colors; when this is between 75% and 90%, it is indicated in light colors.

the structure with two bilayers on top of five QLs Bi_2Se_3, $(Bi_2Se_3)_5(Bi)_4$, is similar to the one where one bilayer is superimposed. When two bilayers are superimposed, 0.043 electrons per unit cell area are transferred, and therefore the binding energy of the top QL Dirac cone further increases.

To illustrate the origin of the different bands in Fig. 2, we examine the evolution of the electronic band structure as a function of the vertical distance between the superimposed Bi bilayer and the Bi_2Se_3 slab, when the bare slab is four QLs thick. The schematic picture of this structure is shown in Fig. 1(b). The results are shown in Fig. 3. First we consider an optimized system of four QLs with one bilayer, relaxing the atomic positions of both the top QL and Bi bilayer, resulting in a bilayer that is located 2.55 Å from the top QL. Next we move the Bi bilayer 4 and 6 Å away from the top surface, while keeping the other relaxed atomic distances of the previous structure. The resulting band structures are shown in Figs. 3(b)–3(d), respectively, where the color scheme of the states is the same as before. The band structure of the single Bi bilayer is shown in Fig. 3(a). Again four Dirac-like cones can be observed for the optimized system in Fig. 3(b), also labeled from 1 to 4, apart from several Rashba-split valence and conduction band quantum-well states. One clearly sees that the binding energy of the top-surface Dirac cone (state 4) increases if the distance to the Bi bilayer decreases, while the Bi bands move upwards due to the increase in charge transfer from the Bi bilayer to the Bi_2Se_3 slab. The bottom-surface Dirac point (state 3) does not change much because the charge-transfer range is short.

The evolution of the bands shows that the Bi bands labeled as 1 in Figs. 2(c) and 3(b) are just ordinary Rashba-split states originating from the built-up dipole due to the charge transfer from the Bi bilayer to the Bi_2Se_3. The Rashba spin splitting in the Bi bands increases upon decreasing the distance to the Bi bilayer, as shown in Fig. 3. We find that the fully relaxed structure has a Rashba splitting of 0.1 eV. Thus, although the Bi bands (state 1) show Dirac-like dispersion at small k in Fig. 3(b), the feature does not remain robust with nonmagnetic impurities as is the case for the original topological surface states of the Bi_2Se_3. The states labeled as 1 in Figs. 2(c) and 3(b), therefore, are *not* topologically protected Dirac states. Our finding does not support the conclusion of Ref. [23] that there exist topological Dirac states localized in the Bi bilayer on Se-terminated Bi_2Se_3. Note that our band structure in Fig. 2(c) agrees with angle-resolved photoemission spectroscopy (ARPES) data [Fig. 2(d)] and the DFT-calculated projected band structure [Fig. 5(e)] in Ref. [13], if we project our bands on the Bi bilayer and the top two QLs as shown in Fig. 4. In Ref. [13], both the range in momentum k in the ARPES data and the energy range in the DFT result, were simply not wide enough to observe the full Rashba splitting. However, there is a significant discrepancy between our band structure, Fig. 2(c), and the DFT-calculated band structure Fig. 3 in Ref. [23]. In the latter, there were no Dirac cones (other than the Rashba-split Bi bands) in an energy range of $(-1.0,0.5)$ eV where we find three Dirac cones (labeled 2–4).

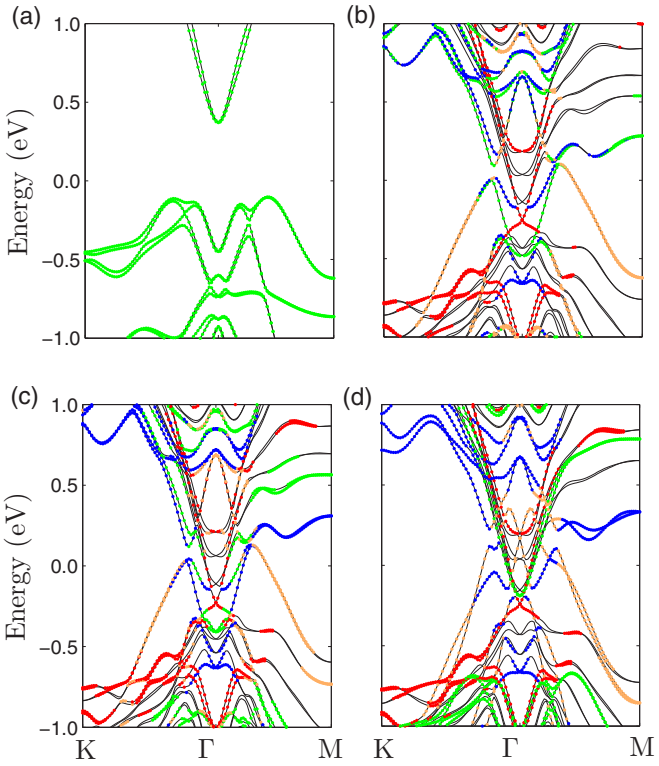

FIG. 5. (Color online) Band structures of (a) a bare one QL, (b) four QLs with a bilayer and a QL on top in the relaxed atomic positions, (c) four QLs with a bilayer on top and a QL at 4 Å and (d) at 6 Å vertical distance.

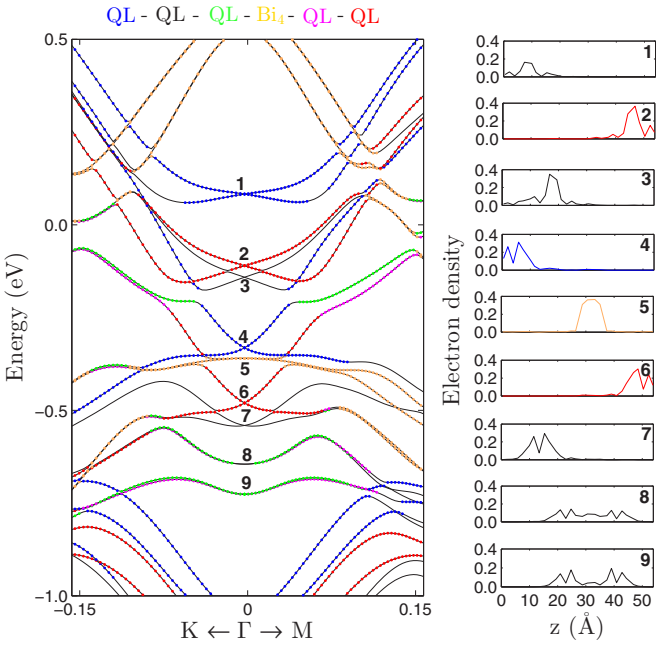

FIG. 6. (Color online) The band structure of a five QL slab with two Bi bilayers inside, which separate two QLs from three QLs. Color coding of the bands is the same as before, with colors for different QLs and the Bi bilayer as shown at the top of the figure. On the right-hand side the layer-projected electron densities of specific states at Γ are shown.

Let us address the origin of the Dirac cone (state 2) in Figs. 3(b) and 2(c). By comparing Figs. 3(b) and 3(c), one observes that the lowest Rashba-split conduction band state in Fig. 3(c) (the case where the Bi bilayer is at a distance of 4 Å from the Bi_2Se_3 slab) has turned into a new Dirac cone in the fully relaxed situation of Fig. 3(b). So if the charge transfer is strong enough, a new Dirac cone appears, originating from a Rashba-split conduction band state. This state is localized slightly deeper in comparison with the original (blue, state 4) top surface cone, as can be seen in Fig. 2(d). In this respect, this result is similar to the case of potassium adsorption on a Bi_2Se_3 surface, considered in Ref. [28].

The emerging Dirac cone was observed in ARPES (Fig. 2D) and in the DFT-calculated projected band structure (Fig. 5E) in Ref. [13]. Note that Fig. 4 in our work agrees with the ARPES data in Ref. [13]. However, the origin of the new Dirac cone was not explicitly mentioned in Ref. [13].

C. Bi bilayers inside Bi_2Se_3

Here we investigate the effect of one or more Bi bilayers inside the Bi_2Se_3 crystal. First, we investigate the evolution of the band structure of the four QL Bi_2Se_3 slab with a Bi bilayer on top, by gradually placing an extra Bi_2Se_3 QL toward the 4QLs + Bi_2, schematically shown in Fig. 1(c). We relax the atomic positions of the topmost QL of the bare four QL slab together with the Bi bilayer and the superimposed QL, resulting in a relaxed structure where the vertical distance between the bilayer and the extra QL is 2.54 Å. The band structure for the fully relaxed case is shown in Fig. 5(b) and the band structures with the extra QL at 4 and 6 Å are shown in Figs. 5(c) and 5(d), respectively, where the other atomic distances are kept fixed. Now the green circles represent states with more than 40% of their density located in this extra QL. For comparison, the band structure of the single superimposed QL is shown in Fig. 5(a). With decreasing distance of the QL on top, the increased charge transfer from the Bi bilayer to this extra QL pushes the Bi bands further upwards, while the green states in the extra Bi_2Se_3 QL move downwards. The charge transfer from the Bi bilayer in both directions makes the internal field disappear, and consequently the Rashba splitting in the Bi bands disappears, as shown in Fig. 5(b). The energy of the blue (top) and red (bottom) Dirac cones of the original four QL slab stays almost unaltered, as well as their localization. The states corresponding to the top (blue) cone are interpreted as topological interface states instead of surface states. We do not observe a topological surface state arising from the superimposed QL, since it is too small.

Since Bi bilayers can also appear deeper inside Bi_2Se_3 crystals, we investigate the electronic structure of a five QL Bi_2Se_3 structure, with one or more Bi bilayer(s) in between, separating the structure in two and three QL slabs, as schematically shown in Fig. 1(d). The band structure for two intermediate Bi bilayers, together with the layer-projected electron densities of specific states at Γ is shown in Fig. 6. Note that only two Dirac cones are present, localized at the topmost QL (state 6) and the bottommost QL (state 4) of the full structure. The Bi bands do not appear near the Fermi level, except for one flat band (state 5). There are three sets

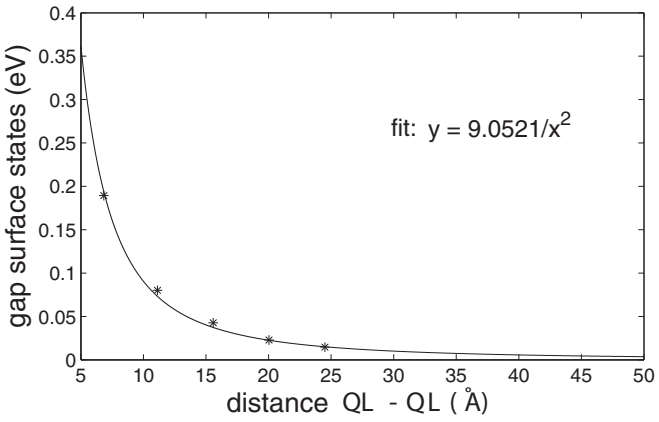

FIG. 7. The gap between the interface states as a function of the distance between the QLs next to the Bi bilayer(s).

of Rashba-split quantum-well states in the bulk conduction band. Two of them can be assigned to the three QLs (states 1 and 3) and the other one to the two QLs (state 2). There is also one set of quantum-well states in the bulk valence band (state 7) localized in the bottom three QLs. The expected interface states coming from the QLs next to the bilayer(s) are apparently missing; however, states 8 and 9 are localized in the region of the two QLs next to the intermediate Bi bilayers. When more bilayers are put in between, these bands come closer, but never form a closed Dirac cone, as can be seen in Fig. 7, where the energy difference between the interface states is shown as a function of the distance between the QLs next to the Bi bilayer(s). The fit shows that the gap closes as $\sim$distance^{-2}, and not exponentially as is the case when a vacuum is created between the two and three QLs. We checked that a vacuum of 10 Å between the two and three QLs is thick enough for the bands to close. However, the gap persists when more Bi bilayers are in between, even though the vertical distance between the two and three QLs is (far) more than 10 Å. Therefore, we conclude that the main reason for the gap, or the reason for a lack of interface states, is the long range character of the interaction between the two QLs via the bilayer(s).

IV. CONCLUSION

To summarize, we examined the influence of Bi bilayers on the electronic structure of the TI Bi_2Se_3 as well as the effect of the TI on the Bi bilayers. Bi_2Se_3 is a good substrate for Bi bilayers, and structures with Bi bilayers combined with Bi_2Se_3 QLs are stable compounds. For Bi_2Se_3(111) slabs, we found that the Bi bilayers do not favor a position inside the slabs or at the surface. First, we investigated the effect of one or two Bi bilayers on top of a Bi_2Se_3 slab, resulting in a charge transfer from the Bi bilayers to the QL slab. We observed increased binding energies of the top-surface and bottom-surface Dirac cones, due to a combination of a structural relaxation effect and the charge transfer, which extends all the way to the bottom QL. The states near the Fermi level coming from the bands of the additional Bi bilayer have been denominated in previous studies to form a Dirac cone, where we found they are just ordinary Rashba-split states originating from the dipole built up by the charge transfer. We also found that an additional Dirac cone emerges due to the charge transfer. This was clearly shown by gradually detaching the extra Bi bilayer from the Bi_2Se_3 slab. Next, we examined the Bi_2Se_3 slab with a Bi bilayer and an extra QL on top, where an increase of charge transfer from the bilayer to the extra QL results in upward and downward movements of the Bi and extra QL bands, respectively, while the original top-surface and bottom-surface Dirac cones remain almost fixed. Moreover, the charge transfer from the Bi bilayer in both directions removes the Rashba splitting in the Bi bands. When the Bi bilayers are located deeper in the Bi_2Se_3 slab, they have the tendency to split the slab into two TIs with well-defined surface states. However, the interface states never close to form a Dirac cone, not even when the number of Bi bilayers is large, due to strong coupling between the neighboring QLs and the Bi bilayers. We conclude that the homologous series of stable structures $(Bi_2)_n(Bi_2Se_3)_m$ can form a wide variety of TI nanostructures, e.g., the surface or interface states can be tuned with the addition or removal of specific QLs or Bi bilayers in order to obtain the desired properties for various applications.

ACKNOWLEDGMENTS

We gratefully acknowledge financial support from the Research Foundation - Flanders (FWO-Vlaanderen). K.G. thanks the University of Antwerp for a Ph.D. fellowship. C.D.B. is an aspirant of the Flemish Science Foundation. This work was carried out using the HPC infrastructure at the University of Antwerp (CalcUA), a division of the Flemish Supercomputer Center VSC, supported financially by the Hercules Foundation and the Flemish Government (EWI Department). K.P. was supported by U.S. National Science Foundation Grant No. DMR-1206354.

[1] M. Z. Hasan and C. L. Kane, Rev. Mod. Phys. **82**, 3045 (2010).
[2] L. Fu, C. L. Kane, and E. J. Mele, Phys. Rev. Lett. **98**, 106803 (2007).
[3] X. Qi and S. C. Zhang, Rev. Mod. Phys. **83**, 1057 (2011).
[4] H. J. Zhang, C. X. Liu, X. L. Qi, X. Dai, Z. Fang, and S. C. Zhang, Nat. Phys. **5**, 438 (2009).
[5] J. Black, E. M. Conwell, L. Seigle, and C. W. Spencer, J. Phys. Chem. Solids **2**, 240 (1957).
[6] D. L. Greenaway and G. Harbeke, J. Phys. Chem. Solids **26**, 1585 (1965).
[7] I. A. Nechaev, R. C. Hatch, M. Bianchi, D. Guan, C. Friedrich, I. Aguilera, J. L. Mi, B. B. Iversen, S. Blugel, P. Hofmann, and E. V. Chulkov, Phys. Rev. B **87**, 121111(R) (2013).
[8] L. Kou, B. Yan, F. Hu, S.-C. Wu, T. O. Wehling, C. Felser, C. Chen, and T. Frauenheim, Nano Lett. **13**, 6251 (2013).
[9] Z. Liu, C.-X. Liu, Y.-S. Wu, W.-H. Duan, F. Liu, and J. Wu, Phys. Rev. Lett. **107**, 136805 (2011).

[10] S. Murakami, Phys. Rev. Lett. **97**, 236805 (2006).
[11] D. Wang, L. Chen, H. Liu, and X. Wang, J. Phys. Soc. Jpn. **82**, 094712 (2013).
[12] Z.-Q. Huang, F.-C. Chuang, C.-H. Hsu, Y.-T. Liu, H.-R. Chang, H. Lin, and A. Bansil, Phys. Rev. B **88**, 165301 (2013).
[13] L. Miao, Z. F. Wang, W. Ming, M.-Y. Yao, M. Wang, F. Yang, Y. R. Song, F. Zhu, A. V. Fedorov, Z. Sun, C. L. Gao, C. Liu, Q.-K. Xue, C.-X. Liu, F. Liu, D. Qian, and J.-F. Jia, Proc. Natl. Acad. Sci. USA **110**, 2758 (2013).
[14] Z. F. Wang, M. Y. Yao, W. Ming, L. Miao, F. Zhu, C. Liu, C. L. Gao, D. Qian, J.-F. Jia, and F. Liu, Nat. Commun. **4**, 1384 (2013).
[15] L. Chen, Z. F. Wang, and F. Liu, Phys. Rev. B **87**, 235420 (2013).
[16] S. H. Kim, K.-H. Jin, J. Park, J. S. Kim, S.-H. Jhi, T.-H. Kim, and H. W. Yeom, Phys. Rev. B **89**, 155436 (2014).
[17] F. Yang, L. Miao, Z. F. Wang, M.-Y. Yao, F. Zhu, Y. R. Song, M.-X. Wang, J.-P. Xu, A. V. Fedorov, Z. Sun, G. B. Zhang, C. Liu, F. Liu, D. Qian, C. L. Gao, and J.-F. Jia, Phys. Rev. Lett. **109**, 016801 (2012).
[18] C. W. Sun, J. Y. Lee, M. S. Youm, and Y. T. Kim, Jpn. J. Appl. **45**, 9157 (2006).
[19] K. Kifune, Y. Kubota, T. Matsunaga, and N. Yamada, Acta Crystallogr., Sect B: Struct. Sci. **61**, 492 (2005).
[20] L. E. Shelimova, O. G. Karpinskii, M. A. Kretova, V. I. Kosyakov, V. A. Shestakov, V. S. Zemskov, and F. A. Kuznetsov, Inorg. Mater. **36**, 768 (2000).
[21] K. Govaerts, M. H. F. Sluiter, B. Partoens, and D. Lamoen, Phys. Rev. B **85**, 144114 (2012).
[22] K. Govaerts, M. H. F. Sluiter, B. Partoens, and D. Lamoen, Phys. Rev. B **89**, 054106 (2014).
[23] X. He, W. Zhou, Z. Y. Wang, Y. N. Zhang, J. Shi, R. Q. Wu, and J. A. Yarmoff, Phys. Rev. Lett. **110**, 156101 (2013).
[24] D. D. dos Reis, L. Barreto, M. Bianchi, Guilherme Almeida Silva Ribeiro, E. A. Soares, W. S. e Silva, V. E. de Carvalho, J. Rawle, M. Hoesch, C. Nicklin, W. P. Fernandes, J. Mi, B. B. Iversen, and P. Hofmann, Phys. Rev. B **88**, 041404(R) (2013).
[25] Y. L. Chen, J. G. Analytis, J.-H. Chu, Z. K. Liu, S.-K. Mo, X. L. Qi, H. J. Zhang, D. H. Lu, X. Dai, Z. Fang, S. C. Zhang, I. R. Fisher, Z. Hussain, and Z.-X. Shen, Science **325**, 178 (2009).
[26] A. A. Kordyuk, T. K. Kim, V. B. Zabolotnyy, D. V. Evtushinsky, M. Bauch, C. Hess, B. Buchner, H. Berger, and S. V. Borisenko, Phys. Rev. B **83**, 081303(R) (2011).
[27] M. Neupane, S.-Y. Xu, L. A. Wray, A. Petersen, R. Shankar, N. Alidoust, C. Liu, A. Fedorov, H. Ji, J. M. Allred, Y. S. Hor, T.-R. Chang, H.-T. Jeng, H. Lin, A. Bansil, R. J. Cava, and M. Z. Hasan, Phys. Rev. B **85**, 235406 (2012).
[28] K. Park, C. De Beule, and B. Partoens, New J. Phys. **15**, 113031 (2013).
[29] G. Kresse and J. Furthmüller, Comput. Mater. Sci. **6**, 15 (1996).
[30] G. Kresse and J. Furthmüller, Phys. Rev. B **54**, 11169 (1996).
[31] J. P. Perdew, K. Burke, and M. Ernzerhof, Phys. Rev. Lett. **77**, 3865 (1996).
[32] J. Klimeš, D. R. Bowler, and A. Michaelides, Phys. Rev. B **83**, 195131 (2011).
[33] H. J. Monkhorst and J. D. Pack, Phys. Rev. B **13**, 5188 (1976).
[34] Y. Zhang, K. He, C. Z. Chang, C. L. Song, L. L. Wang, X. Chen, J. F. Jia, Z. Fang, X. Dai, W. Y. Shan, S. Q. Shen, Q. Niu, X. L. Qi, S. C. Zhang, X. C. Ma, and Q. K. Xue, Nat. Phys. **6**, 584 (2010).
[35] W. Zhang, R. Yu, H. J. Zhang, X. Dai, and Z. Fang, New J. Phys. **12**, 065013 (2010).
[36] O. V. Yazyev, J. E. Moore, and S. G. Louie, Phys. Rev. Lett. **105**, 266806 (2010).
[37] L. Kou, S.-C. Wu, C. Felser, T. Frauenheim, C. Chen, and B. Yan, ACS Nano (2014), doi:10.1021/nn503789v.
[38] C. Li, T. Winzer, A. Walsh, B. Yan, C. Stampfl, and A. Soon, Phys. Rev. B **90**, 075438 (2014).
[39] K. Park, J. J. Heremans, V. W. Scarola, and D. Minic, Phys. Rev. Lett. **105**, 186801 (2010).